

Strain relaxation during the initial stages of growth in Ge/Si(001)

A. A. Williams, J. M. C. Thornton, and J. E. Macdonald

Department of Physics, University of Wales College of Cardiff, P.O. Box 913, Cardiff CF1 3TH, United Kingdom

R. G. van Silfhout and J. F. van der Veen

*FOM Institute for Atomic and Molecular Physics, Kruislaan 407,
1098 SJ Amsterdam, The Netherlands*

M. S. Finney, A. D. Johnson, and C. Norris

Department of Physics, University of Leicester, Leicester LE1 7RH, United Kingdom

(Received 20 September 1990)

Grazing-incidence x-ray diffraction has been utilized to give a direct measure of the lateral strain distribution during *in situ* molecular-beam epitaxy deposition of Ge onto Si(001). The results demonstrate that the critical thickness for strain relaxation is 3–4 monolayers (ML), which coincides with that at which islanding is observed. Strain relief is gradual and depends strongly on growth conditions and annealing procedure. At a coverage of ~ 10 ML the strain distribution exhibits two components, one of which is almost fully relaxed and the other having a range of lattice spacings intermediate between those for bulk Si and Ge. Concurrent specular reflectivity measurements have been used to monitor intermixing at the interface, showing that the island formation onset is at 3–4 ML, with a rapid increase in island height beyond a coverage of 6 ML. Comparison with electron-microscopy results indicates that strain relaxation is intimately related to islanding on the Ge surface.

I. INTRODUCTION

In recent years, considerable effort has been directed towards the study of heteroepitaxial semiconductor growth. This has been both in order to understand the fundamental nature of interface formation, and also to approach the fabrication of a new range of novel, strained-layer device structures. Such structures are of particular interest because the introduction of both artificial periodicity and strain into the material can significantly alter the electronic band structure. By considering crystal growth, therefore, the material band structure may be engineered to optimize the desired device performance. In the case of Si/Ge superlattices, a major current goal is the ability to transmute the electronic band structure of the elements, which have indirect band gaps, to one which has a quasidirect form, thus permitting its use in optoelectronic devices. Indeed, the direct optical transitions which result from modified band structures of this kind have been reported by several authors.^{1,2}

One of the limiting factors in the growth of semiconductor heterojunctions is the critical thickness of the overlayer. Even in near lattice-matched cases, the difference in lattice parameter of the two constituents leads to increasing strain energy in the overlayer as pseudomorphic growth proceeds. At the critical thickness, this strain energy is released, with the in-plane lattice parameter of the overlayer assuming a value closer to that it would have in the bulk crystal. Most studies of strain relaxation have concentrated on materials which are close to being lattice matched, where the critical thickness is

relatively large. In this regime, the relaxation mechanisms are fairly well understood in that dislocations form and propagate throughout the overlayer. This critical thickness may be calculated by considering the balance of energy or of mechanical forces on dislocations.^{3–5} Experimental data were found to support much larger critical thicknesses than the predicted values from these models.⁶ It was pointed out by Fritz and others, however, that techniques such as x-ray diffraction and ion scattering were not sufficiently sensitive to detect the onset of strain relief, giving rise to artificially high values of the critical thickness.⁷ Annealing studies also established the role of thermal treatment on strain relief and demonstrated that it is a kinetically driven process.⁸ The use of techniques which detect dislocations directly, coupled with anneals at temperatures high enough to attain the equilibrium state, yield values of the critical thickness in very close agreement with the models of Matthews and Blakeslee.⁹

In more highly strained systems, where the lattice parameters have a greater difference, the relaxation mechanisms have often been assumed to be of similar nature, leading to a corresponding decrease in the critical thickness. It is well known, however, that three-dimensional islands form after only a few monolayers of overgrowth with the Ge on Si system. This behavior has been explained by the possibility that strain in the overlayer can be reduced by the formation of interfacial misfit dislocations, under the islands.¹⁰ This Stranski-Krastanow growth mode¹¹ differs from the Volmer-Weber mode, where islands form on the substrate immediately on deposition.¹² More recently, it has become apparent that the

initial stages of this relaxation mechanism may be yet more complicated by the introduction of elastic strain into the overlayer and islands,¹³ and it is this initial behavior which this study seeks to address.

In order to gain a more complete understanding of strained overlayer systems, it is therefore desirable to investigate both strain and morphology as the layer relaxes. The latter is probed very effectively with transmission electron microscopy (TEM), scanning electron microscopy (SEM), and scanning tunneling microscopy (STM). Oscillations in the intensity of the diffracted beam in reflection high-energy electron diffraction (RHEED) is also used to monitor the transition from two-dimensional (2D) to three-dimensional (3D) growth during deposition, but less care is sometimes taken to ensure that the surface has not islanded after deposition is complete. This is important as it is known that islands cluster by mass transport from smaller islands to larger islands, a process referred to as Ostwald ripening.¹⁴ This clustering process is again enhanced by thermal annealing and therefore it should not necessarily be assumed that islanding does not occur on the basis that layer-by-layer growth is observed during deposition. Whereas the above techniques provide local probes of the surface morphology, they do not give a high-resolution measurement of interatomic spacing and strain. For thicker overlayers, strain is usually characterized by x-ray diffraction. The low flux of laboratory sources, coupled with the low scattering cross section for x-rays, mean that x-ray diffraction is not used to study heavily strained systems, where the critical thickness is on the monolayer scale. Apart from the intensity limitations, the conventional diffraction geometry entails a very low overlayer-to-bulk ratio of the diffracted intensities, which would make studies using even synchrotron radiation difficult to perform. Strain in such ultrathin layers has been measured with electron diffraction^{15–17} and ion scattering.^{18,19} In this paper we demonstrate that x-ray diffraction using synchrotron radiation and employing a grazing-incidence geometry provides superior resolution and sensitivity for studying strain relief in monolayer-thick films, and apply it to the investigation of the Ge/Si(001) system. This technique has also been used for an earlier study for this system²⁰ and for the case of GaAs/Si(001) which displays contrasting behavior.²¹ With the capability to measure both diffracted and reflected x rays, this technique can provide information concerning the strain and morphology in the surface region, thus making it especially powerful in the study of these types of material systems.

With regard to germanium overlayers on Si(001), many independent studies have shown by various means that, for growth temperatures above about 350°C, the overlayer forms in the Stranski-Krastanow mode, with islanding occurring after 3–4 ML of uniform deposition²² (1 ML=1.41 Å). Auger spectroscopy²³ and electron diffraction²² provide less direct evidence for the islanding process, whereas TEM and SEM provide direct images of the islands and show their evolution with time and annealing temperature.²⁴ Islanding of the overlayer surface also occurs on annealing after room-temperature deposition.²⁵ Eaglesham and Cerullo¹³ have used TEM to ob-

serve that the islands formed during deposition at 500°C are dislocation-free for island heights of up to 500 Å, well in excess of the predicted critical thickness for dislocation formation, which is in the region of 10–20 Å.⁴ This is a strong indication that the strain energy is initially relieved by the formation of the islands, in which the Ge interatomic separation can be closer to that in bulk Ge. Eaglesham and Cerullo interpret the contrast in their images as an elastic deformation of the crystal around the islands and they estimate that the strain could thus be reduced from 4% to 2.5%. This deformation takes the form of curvature of the crystal planes, to which x-ray diffraction is sensitive through the width of the measured Bragg peaks, whereby a variation in the crystal-plane orientation results in a broadening of the Bragg peak. The stability of the initial uniform Stranski-Krastanow layer and the clustering kinetics of 3D growth at higher coverages have been studied using electron microscopy and ion scattering.²⁴ Recent work by Mo *et al.*²⁶ using STM has shown that a 3D cluster phase exists between layer-by-layer growth and macroscopic islanding of Ge on Si. These “hut clusters,” which are seen after Ge coverages of greater than 3 ML, are faceted and specifically oriented, though it is not clear as to whether they are strained or relaxed from the STM data. This last point is of great importance in understanding the overall relaxation process of Ge on Si.

Few studies have quantified the strain in Ge overlayers on Si(001) and thus monitored the strain relief process as it occurs. Ion scattering¹⁸ and RHEED (Ref. 15) studies have detected the onset of strain relaxation at a coverage of 6 ML, with full relaxation occurring at coverages greater than 10 ML. This behavior contrasts with the onset of islanding at a 3-ML coverage, and so indicates that strain relief sets in only after appreciable islanding has already occurred, and also that the islands do not in themselves lead to appreciable strain relief. Ion scattering and RHEED, however, are less sensitive to small changes in atomic spacing than x-ray diffraction. We therefore aim to exploit the superior resolution of x-ray diffraction to determine the onset of strain relaxation and to determine the detailed distribution in the Ge overlayer. By employing a variety of growth conditions we also attempt to show the effects of growth conditions and thermal treatment on the strain distribution. Concurrent specular reflectivity measurements are also performed for one sample to characterize interface and surface morphology.

II. EXPERIMENTAL TECHNIQUE

Grazing-incidence x-ray diffraction has now been used for a number of years to determine the atomic structure of reconstructed surfaces.²⁷ In this geometry, the incident and scattered beams subtend small angles (< 1°) to the crystal surface. The beam penetration may be limited to ≈ 50 Å by reducing these angles to below the critical angle for total external reflection. When coupled with the high flux of synchrotron sources, this scattering geometry offers many benefits for studies of strain relaxation in ultrathin films, as outlined below.

For a strained, unrelaxed layer, the lattice parameter of the epilayer and the substrate are identical in the plane of the interface, thus causing a tetragonal distortion of the epilayer unit cell. As the layer relaxes, its in-plane lattice parameter increases towards its bulk value and the tetragonal distortion is reduced, thus changing the lattice parameter normal to the interface as illustrated in Fig. 1. Conventional x-ray diffraction studies of strained layers primarily involve scans of the scattering vector Q_{\perp} normal to the surface, the in-plane component Q_{\parallel} being small or zero. Consequently strain relaxation is detected as a shift in the epilayer peak as the tetragonal distortion is relieved. In the grazing-incidence geometry, both incident and diffracted beams are close to the plane of the interface and thus $Q_{\perp} \approx 0$. The strain distribution is probed by scanning radially outwards in reciprocal space (the so-called ϑ - 2ϑ scan) through the region around a substrate Bragg peak. In this geometry, the peak from an unrelaxed epilayer coincides with that of the substrate as a result of their identical in-plane lattice spacings. Any relaxed material having an in-plane spacing different from the substrate value gives rise to a separate peak and thus relaxation in small localized regions of the epilayer may be detected, even when the rest of the layer is fully strained. This contrasts with the conventional diffraction geometry where the peak from the unrelaxed material

would dominate the data. This feature provides superior sensitivity to limited strain relaxation when compared to ion scattering and other techniques which are applicable to ultrathin films. The grazing-incidence geometry also benefits from a much narrower intrinsic peak width for the epilayer due to the much larger extent and coherence of the film parallel to the interface than normal to it. This allows the strain distribution to be measured directly with good resolution. The scattering from the substrate crystal truncation rod,²⁸ which can obscure the epilayer peak in the conventional geometry, may also be resolved entirely and consequently does not obscure the epilayer scattering. The limited beam penetration of the grazing-incidence geometry also suppresses the thermal diffuse scattering from the bulk crystal which gives rise to troublesome scattering near the base of bulk Bragg peaks, thus obscuring the scattering from slightly relaxed material.

The experiments were performed using unfocused radiation from the Wiggler beamline at the Synchrotron Radiation Source in Daresbury (U.K.). The x rays were monochromated using the (111) reflection from a channel-cut silicon crystal. For sample I, an incident-beam wavelength of 0.80 Å was used, giving a critical angle for total reflection in Si of 0.12°. For samples II, III, and IV the wavelength was 1.38 Å, giving a critical angle of 0.20°. The incident and exit grazing angles used for the x-ray beam were set at $\beta=0.09^\circ$ and $\beta'=0.13^\circ$, respectively, for sample I, and $\beta=0.08^\circ$, $\beta'=0.09^\circ$ for samples II and III. The incident beam was defined by slits of $0.1 \times 3.0 \text{ mm}^2$ at a distance of 40 m from the source, giving a high degree of collimation. The detector aperture subtended an angle of 0.10° at the sample.

The equipment consists of a large five-circle diffractometer, connected to an ultrahigh vacuum chamber with *in situ* molecular-beam epitaxy (MBE) growth, as well as standard surface-science techniques.²⁹ The use of a five-circle diffractometer rather than an ordinary four-circle diffractometer enlarges the accessible range of momentum transfer and allows the surface normal to lie in the horizontal plane during scans. The Si(001) substrates were cleaned by light sputtering with 800-eV Ar^+ ions for 60 s followed by an anneal for 3 min at 1060 °C. This gave a sharp (2×1) diffraction pattern, observed with RHEED and x-ray diffraction. The full width at half maximum (FWHM) of the $(\frac{3}{2}, 0)$ and $(0, \frac{3}{2})$ fractional order reflections, arising from the double domain (2×1) reconstruction, were $\approx 0.02^\circ$ for the clean surface, corresponding to an average reconstructed domain size of $\sim 7000 \text{ \AA}$.

The sample physical surface normal was aligned by reflection of a laser beam, while the crystallographic alignment was determined from the position of four bulk reflections.²⁸ The miscut of the surface relative to the [001] crystallographic axis was thus determined to be 0.04° . The real unit-cell vectors, used to define the scattering vector $\mathbf{Q} = h\mathbf{b}_1 + k\mathbf{b}_2 + l\mathbf{b}_3$ in reciprocal space may be related to the conventional bulk cubic real-cell vectors by $\mathbf{a}_1 = (1, 1, 0)_{\text{cubic}}$, $\mathbf{a}_2 = (1, -1, 0)_{\text{cubic}}$, and $\mathbf{a}_3 = (0, 0, \frac{1}{4})_{\text{cubic}}$.

X-ray reflectivity provides a measure of the electron-

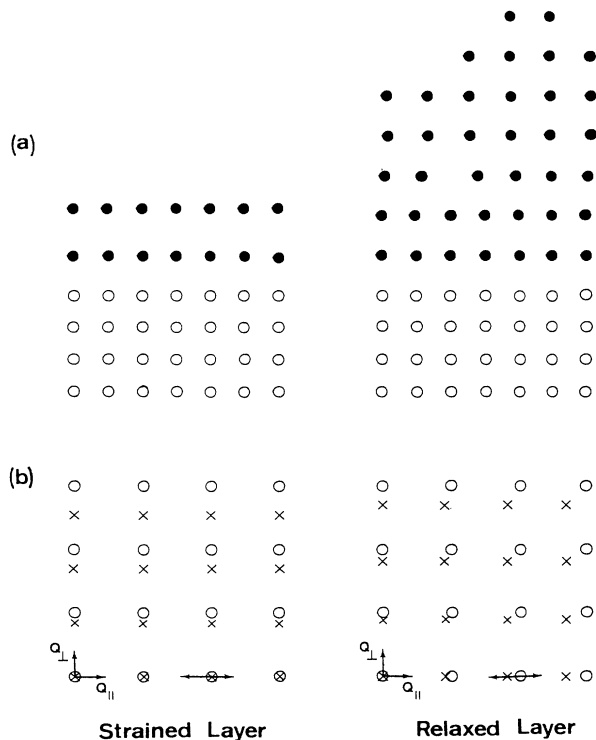


FIG. 1. A schematic side view of (a) direct space and (b) reciprocal space for a fully strained and partially relaxed layer. In (a), the open and solid circles denote substrate and epilayer atoms, respectively. In (b), the open circles and crosses denote the substrate reciprocal-lattice points and the peak position for the substrate and fully relaxed epilayer, respectively. A radial scan at grazing incidence is denoted as an arrow.

density distribution as a function of depth. In this case, the aim of the measurements was to mark the onset of islanding of the surface and to probe the degree of intermixing at the Ge/Si interface. The specular reflectivity was measured for sample I, for most investigated coverages, concurrently with the radial scans, the experimental conditions being identical to those given above.

Following an earlier preliminary study,²⁰ four samples were investigated in order to study the effect of thermal treatment on the relaxation process. These are denoted as follows.

Sample I. The substrate was held at 550°C during deposition and then immediately cooled to room temperature before measurement. This procedure was repeated after deposition of each monolayer.

Sample II. The substrate was maintained at 520°C during deposition and the subsequent measurements.

Sample III. A deposition of 2 ML of Ge was made onto a substrate held at a temperature of 320°C. This was to avoid any intermixing at the interface, which has been suggested by a Raman-scattering study.³⁰ Following this came an anneal at 520°C for 30 min. Measurements were then performed at room temperature and this procedure was repeated for each subsequent deposition of 1 ML.

Sample IV. Samples of varying thickness prepared by MBE at British Telecom Research Laboratories. The Ge was deposited onto the substrates at a rate of 0.5 \AA s^{-1} and at a temperature of $400 \pm 50^\circ\text{C}$. The samples were then capped with amorphous Si and the experiment performed in air. For samples I, II, and III, Ge was deposited at a rate of 1 ML per 18 min, using a Knudsen effusion cell calibrated by Rutherford backscattering. A comparison of the results with those of sample IV thus give an

indication of the effect of a 500-fold increase in the growth rate.

III. RESULTS AND DISCUSSION

A. Diffraction

Radial scans along the b_1 direction in reciprocal space were performed across the (2,0) Bragg peak for all of the samples, the results of which may be seen in Figs. 2–6. This type of scan is sensitive to the distribution of lattice spacings parallel to the interface, and therefore probes the in-plane strain of the overlayer. The resolution along h , determined by the detector aperture slits and the illuminated surface area, was 0.02 reciprocal lattice units (r.l.u.). Figure 2 shows that the peak profile for sample I remains unchanged for a coverage of $\Theta \leq 3$ ML. This is direct evidence that the Ge initially grows pseudomorphically with an in-plane lattice spacing identical to the Si substrate. At a coverage of 3.2 ML the base of the Bragg peak becomes slightly asymmetric, which becomes more noticeable at 3.9 ML where a weak shoulder is seen to develop. This may be attributable to the onset of strain relaxation in the germanium.

This is a highly significant result, since not only does this onset occur at a considerably reduced overlayer thickness when compared to previous work,^{15,17} but it also coincides with the well-reported onset of overlayer islanding.^{22,23} The growth of Ge on Si(001) is known to proceed through the Stranski-Krastanow mode, where islands form on the surface of the Ge at a coverage of around 3 ML. This concurrence indicates that the onset of strain relaxation relates to the formation of islands rather than the generation of misfit dislocations. There is

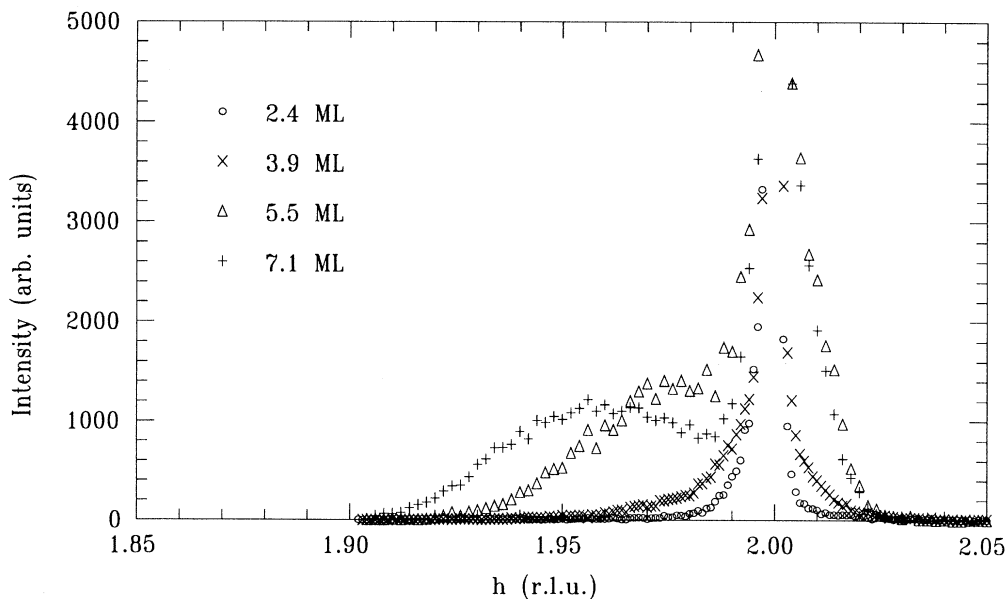


FIG. 2. Radial scans as a function of coverage for sample I. The intensity is plotted on an arbitrary scale. On this scale, the Bragg-peak intensity is $\sim 10^5$ units. Notice the slight increase in asymmetry in the 3.9-ML peak when compared with the one corresponding to a 2.4-ML coverage, which shows the onset of relaxation in the overlayer.

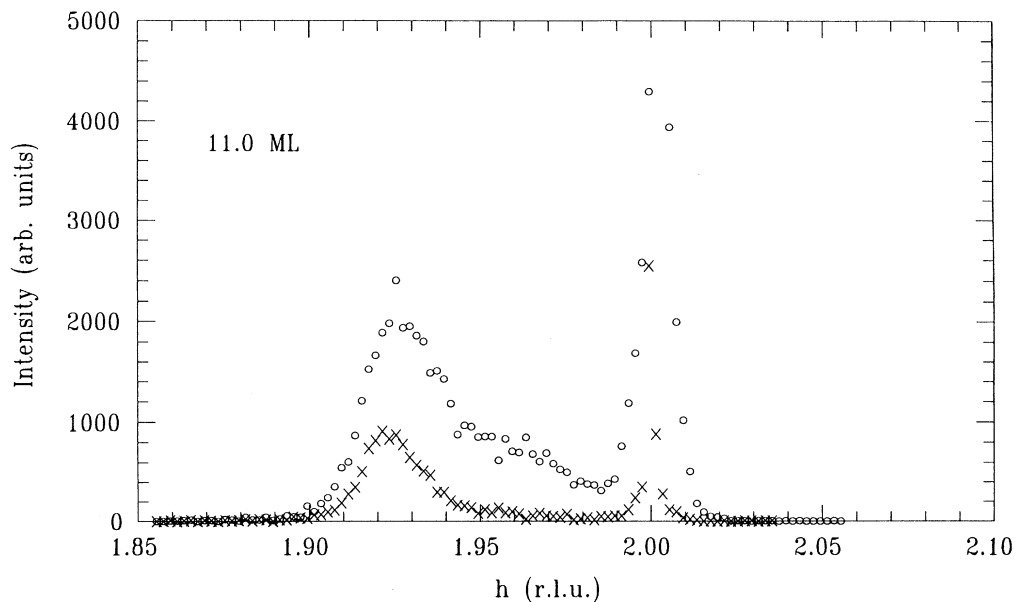


FIG. 3. Radial scans for sample I, with a coverage of 11 ML. Circles denote data for $\beta=0.09^\circ$, $\beta'=0.13^\circ$ and crosses represent the same scan with $\beta=0.07^\circ$, $\beta'=0.05^\circ$, leading to a reduced penetration depth. This shows the partially relaxed material to be near to the interface, rather than at the surface.

also some evidence for the curvature of the crystal planes due to an elastic deformation associated with the islands. It is best seen in Fig. 7, where the radial scans corresponding to coverages of 2.4 ML and 5.5 ML are plotted for comparison on a logarithmic intensity scale. A broad base to the Bragg peak obtained with a 5.5-ML coverage

is clearly visible, which may be attributable to a deformation of the surface region. A characteristic radius of curvature r_c for this deformation may be determined, which in this case is $\approx 30 \mu\text{m}$ (assuming an island diameter of $\approx 1000 \text{ \AA}$). This value also concurs with recent TEM observations of dislocation-free islands in Ge/Si(001) for is-

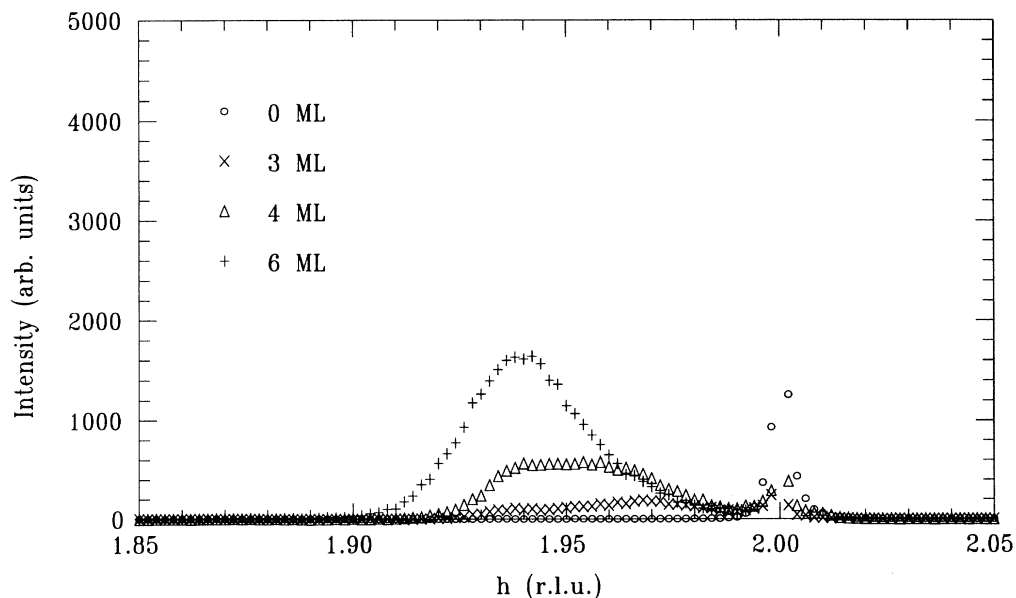


FIG. 4. Radial scans as a function of coverage for sample II. These show how an increased time at high temperature (520°C) leads to an increased rate and more complete relaxation in the overlayer.

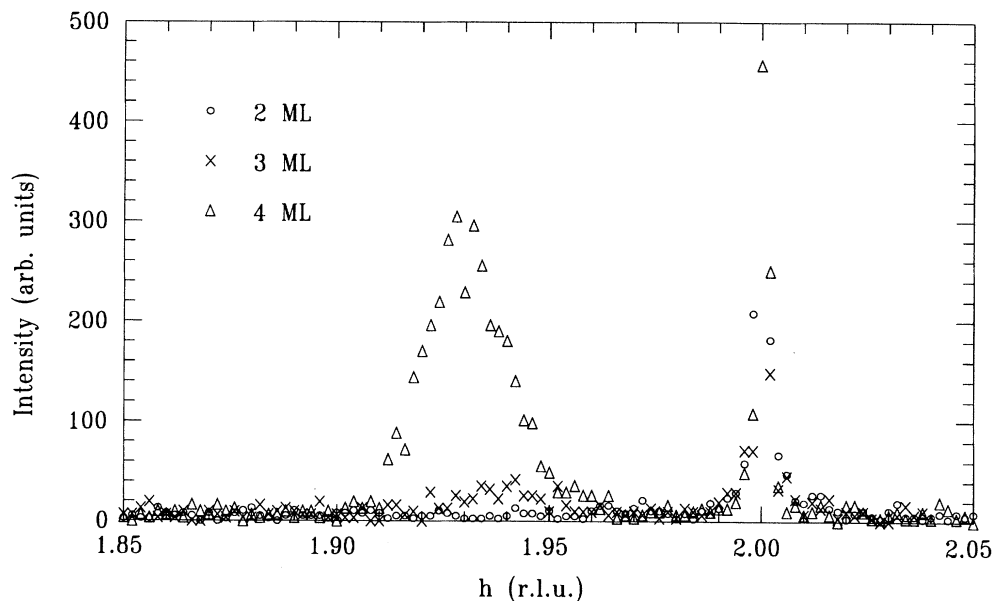


FIG. 5. Radial scans as a function of coverage for sample III. These show only a limited quantity of relaxed material after growth at 320°C, though a more complete relaxation to bulklike Ge has occurred. This is possibly due to nucleation of “bulk” Ge around defects in the overlayer, which may be expected after such a low temperature growth.

land heights of hundreds of Ångströms.¹³ However, further scans of other reciprocal-lattice points would be required to test the possibility.

With increasing overlayer coverage, the partially relaxed component due to germanium shifts to lower values of h , until at a coverage of 11 ML it adopts the position expected for bulk germanium ($h = 1.92$ r.l.u.). This is in

agreement with the RHEED and ion-scattering work mentioned earlier, which reported the observation of completely relaxed germanium at a coverage of ≈ 10 ML.¹⁵ Additional information is obtainable from the intermediate reciprocal-lattice space, since this contains the detailed strain distribution within the developing overlayer.

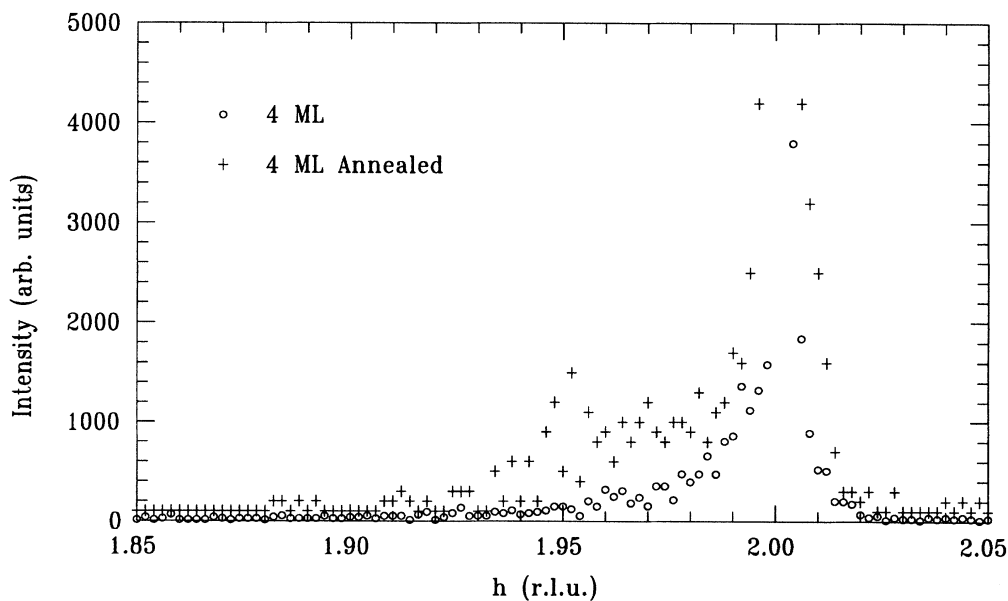


FIG. 6. Radial scans before and after annealing a 4-ML Ge coverage on sample IV, which was grown at 0.5 \AA s^{-1} . These show that no significant difference in the relaxation of the Ge overlayers is seen even if the growth rate undergoes a 500-fold increase.

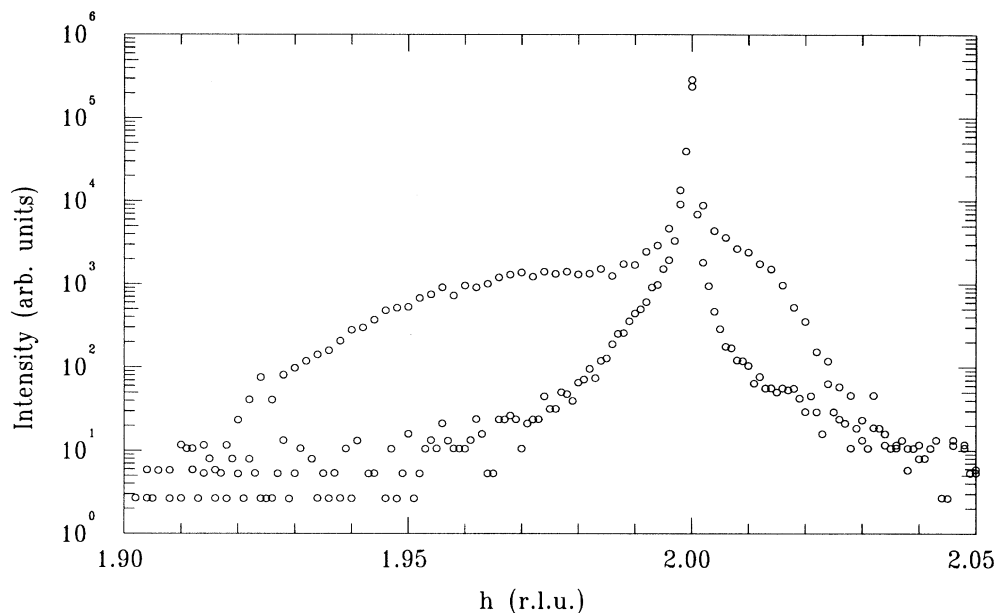


FIG. 7. Radial scans of the coverages of 2.4 and 5.5 ML plotted on a logarithmic intensity scale to show difference in their base widths. This may be attributed to elastic deformation of the substrate around the Ge islands.

For overlayer coverages of 5.5 and 7.1 ML, the germanium partially relaxes, with peaks centering at $h = 1.97$ and 1.95 r.l.u., respectively. The fact that the germanium is not seen to relax fully at this stage lends support to the argument that the initial relaxation mechanism is one where deformation through islanding occurs. Even when fully relaxed germanium is observed for the 11-ML coverage, a not insignificant proportion of the total signal is found at values of reciprocal space corresponding to intermediate strain in the overlayer. The question arises whether the strain is distributed laterally across the overlayer, or as a function of distance from the interface.

In order to probe this further, radial scans for the 11-ML coverage sample were repeated with $\beta = 0.07^\circ$ and $\beta' = 0.05^\circ$, thereby ensuring that the detected beam was entirely below the critical angle. The scattering depth³¹ was thus reduced from 100 \AA to 40 \AA and led to the scan profile denoted by crosses in Fig. 3. In this case, the scattered intensity from the "plateau," in the region $h = 1.95\text{--}2.00$ r.l.u. has been strongly attenuated relative to the peak at $h = 1.92$ r.l.u., indicating that the atomic layers closest to the interface are still strained while the surface layers are almost fully relaxed. It should be noted that the values of the scattering depth quoted above are difficult to interpret in view of the islanding that occurs at this coverage, since a significant fraction of this beam may be totally externally reflected from the tops of islands, thus shadowing parts of the surface. It should also be noted that from 5.5 ML onwards, there is a decrease in the scattered intensity from the intermediate area, around $h = 1.98$ r.l.u., suggesting that the relaxation in the Ge occurs through a continuous release of strain as the coverage increases.

The relaxation process seen here for germanium should be compared with recent similar work on the GaAs/Si(001) system.²¹ In contrast to the Stranski-Krastanow growth observed for germanium, where only the Bragg peak due to silicon and strained germanium was observed, the GaAs was seen to form as partially relaxed material immediately on deposition. This is indicative of immediate islanding of the GaAs, showing that the overlayer forms through the Volmer-Weber growth mode. This is entirely consistent with RHEED observations of initial GaAs/Si growth.³² The development of the area of the relaxed material with coverage is also informative with regard to the nature of the strain distribution within the overlayer. In the case of the GaAs/Si system, the area of the relaxed material increases roughly linearly with the coverage, showing that nearly all of the overlayer is in some way relaxed. For Ge/Si, however, the relaxed area does not increase rapidly until a coverage of about 5 ML is reached. This suggests that even when some islanding of the germanium has occurred (from ≈ 3 ML) an incomplete relaxation exists, with the remainder overlayer still being strained.

Transverse scans (along \mathbf{k}) were employed to determine the extent of correlations laterally across the surface for both fully relaxed and partially relaxed regions at 11 ML. After correction for resolution effects and assuming isotropic correlations in two dimensions, the FWHM at $h = 1.92$ and 1.97 r.l.u. result in correlation lengths of 80 and 100 \AA for the relaxed and partially relaxed regions, respectively. The detailed interpretation of these values of the correlation lengths in terms of parameters such as dislocation densities is unclear at present. Radial scans were performed around $(h, k) = (\frac{3}{2}, 0)$ and $(0, \frac{3}{2})$ to search for any fractional orders in the diffracted beams from the

overlayer. They were indeed found to be present for germanium coverages up to 5 ML, though they were rather weak in intensity. This shows that up to a 5-ML coverage, areas of the overlayer surface are present in a (2×1) reconstruction, following the structure of the initial silicon substrate surface.

For sample II the temperature was maintained at 520°C throughout the growth and measurements and the resulting scans are shown in Fig. 4. At a coverage of 3 ML, the sample has relaxed far more than at the same stage with sample I, and shows a wider range of lattice spacings, from $h = 1.93$ – 2.00 r.l.u. This may indicate that the Ge in sample I has not fully relaxed and at a prolonged elevated substrate temperature the Ge would relax further. This would also explain the decrease in the scattered intensity in the intermediate area at $h = 1.98$ r.l.u., as the Ge coverage increases. At 6 ML the strain is reduced to about 1%, with a peak forming at $h = 1.94$ r.l.u. The scattered intensity at $h = 1.98$ r.l.u. remains constant from 3 to 6 ML, indicating that although there is still an intermediate region of scattered intensity between the two peaks, the Ge at each coverage has finished relaxing.

The radial scans for sample III are shown in Fig. 5, and were performed at room temperature after deposition at 320°C followed by an anneal at 520°C. At 3 ML an extremely weak peak in intensity appears, before becoming more prominent at a coverage of 4 ML. The peak appears at the almost fully relaxed position of $h = 1.93$ r.l.u. and is much weaker than the scattered intensity observed in the earlier samples, indicating that very little of the Ge relaxes. There is also no intermediate intensity between the two peaks, showing that the Ge almost fully relaxes into localized bulklike Ge islands, possibly nucleating at defects induced by the low-growth temperature, instead of a continuous relaxation as seen in earlier samples.

Sample IV was prepared with a more rapid MBE growth by British Telecom in the form of 4 ML of germanium deposited onto Si(001), before capping with amorphous silicon. The radial scans resulting from this material can be seen in Fig. 6. A comparison of the annealed (for 30 min at 500°C) (circles) and nonannealed (crosses) samples show that the Ge partially relaxes even before annealing, and then continues to relax after further thermal treatment. This is consistent with the earlier samples and the clustering of islands observed by Zinke-Allemang, Feldman, and Nakahara.¹⁴

B. Reflectivity

Work done using Raman scattering and ion scattering shows that when Ge is deposited at substrate temperatures of greater than 250°C, some intermixing occurs at the interface.¹⁹ In an attempt to determine the extent of intermixing and surface roughness, specular reflectivity scans were performed concurrently with the radial scans on sample I. For specular reflection, the wave-vector transfer Q is given by $Q = 2k \sin\theta$, where $k = 2\pi/\lambda$ and θ is the angle of incidence and exit.

Several models of the density profile perpendicular to the surface involving two roughened interfaces, were em-

ployed to fit the data. These were found to be inadequate to account for the data for coverages greater than 3 ML. A model involving a uniform layer of Ge with an island on top was introduced to simulate the actual physical picture for Stranski-Krastanow growth. The reflected amplitude was calculated by considering the scattering from discrete atomic layers,

$$I = \frac{S}{Q^2} \left| F_{\text{Si}}(Q) \frac{1}{1 - e^{-Qa_{3\text{Si}}}} + \sum_{n=1}^N c_n F_{\text{Ge}}(Q) e^{iQna_{3\text{Ge}}} \right|^2,$$

where F_{Si} and F_{Ge} are the structure factors for Si and Ge, respectively; $a_{3\text{Ge}}$ ($\approx 1.04a_3$) is the lattice vector perpendicular to the interface. S is a scaling factor, and Q^{-2} includes the area correction and Lorentz factor.³³ The factor c_n for the fractional coverage of layer n is introduced to enable simulation of island formats and is defined by

$$c_n = \begin{cases} 1, & n \leq N_{\text{SK}} \\ f_1 + \frac{(f_2 - f_1)(n - N_{\text{SK}}^{-1})}{(N - N_{\text{SK}})}, & n > N_{\text{SK}} \end{cases}$$

where f_1 is the initial fractional coverage for the lowest atomic level of the island, f_2 is the fractional coverage of the highest atomic island, and N_{SK} is the thickness of the Stranski-Krastanow layer. The value of f_2 was determined from N_{SK} and N_k , with f_1 following these in order to maintain the total germanium coverage. The factor c_n for atomic layers near the Ge/Si interface and at the island surface was modified to include a Gaussian roughening of the Si/Ge interface. This simulates a density profile shown schematically in Fig. 8. Clearly, such a simple model involving a linearly varying fractional coverage cannot fully account for the real physical situation involving a distribution of island heights and widths.

The three fitted models of the electron density profile were as follows.

- Layer-by-layer (Frank–van der Merwe³) ($N_i = 0$).
- Islanding (Volmer-Weber¹²) ($N_{\text{SK}} = 0$).
- Layer plus islands (Stranski-Krastanow¹¹).

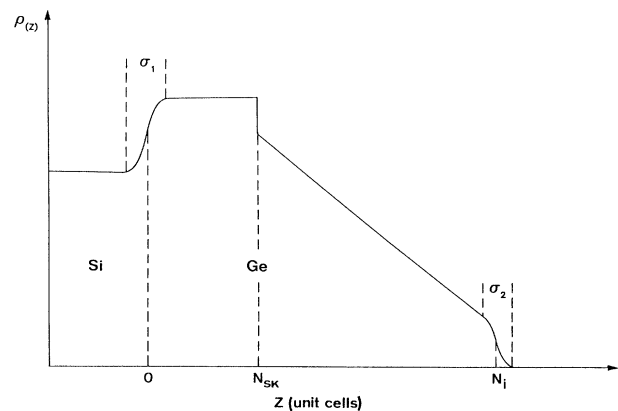


FIG. 8. The profile of the electron density perpendicular to the sample surface ($\rho_{(z)}$) used to model the reflectivity expected from a surface form in the Stranski-Krastanow mode. The perpendicular distance is determined by the number of unit cells from the Si/Ge interface.

The best fits using a χ^2 agreement factor for various coverages of the model simulating Stranski-Krastanow growth are compared in Fig. 9 to the best fits of the two other models, one with no islanding and the other with no Stranski-Krastanow layer. N_k and N_{SK} were fixed and the remaining parameters fitted, followed by iteration with new values of N_k and N_{SK} . The error on these values is within 1 ML up to 5.5 ML. The resulting values for σ_1 and σ_2 show a fair degree of scatter, but they still allow an interfacial roughness in the order of 1 to 2 ML to be determined over the coherence length of ≈ 1000 Å. Information obtained on the degree of intermixing and surface roughness was found to be inconclusive. Up to 2.4 ML, the fitted model suggests that although the surface may roughen, no islanding seems to occur. After 3 ML, model (c) increasingly gives a better fit as judged by the χ^2 values, although up to 5.5 ML the height of islands is still relatively small. At 7 ML the island height N has increased significantly to ≈ 100 ML (Fig. 10), the fit being rather insensitive to larger values of N_k . An island height of greater than 500 ML as suggested by TEM (Ref. 13) would be compatible with this fit. The fitted Stranski-Krastanow layer thickness N_{SK} increases with coverage from 3 ML at a coverage of 4.7 ML, to 5 ML at a coverage of 7 ML, suggesting that it continually develops with increasing coverage. Nevertheless, it should be stressed that the reflectivity data does indicate the overall behavior, but the resulting values of the parameters

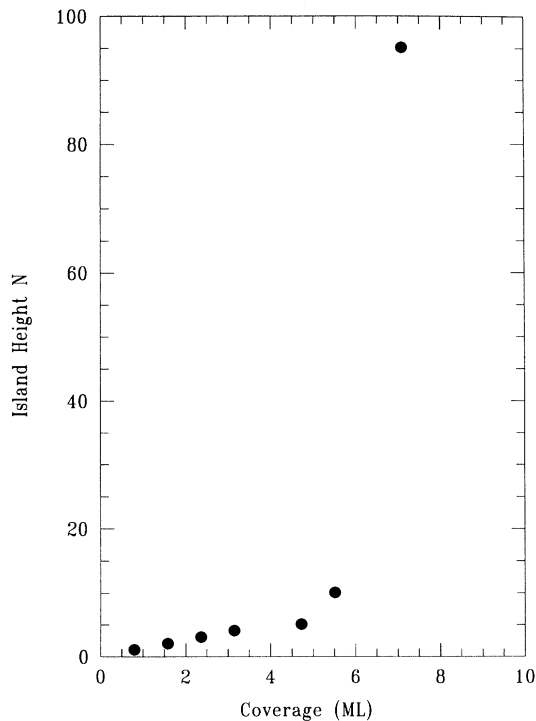


FIG. 9. Graph to show the growth of Ge island height (in number of unit cells) as a function of total (deposited) coverage. Note the nonlinearity and the sudden increase in island height at ~ 6 -ML coverage.

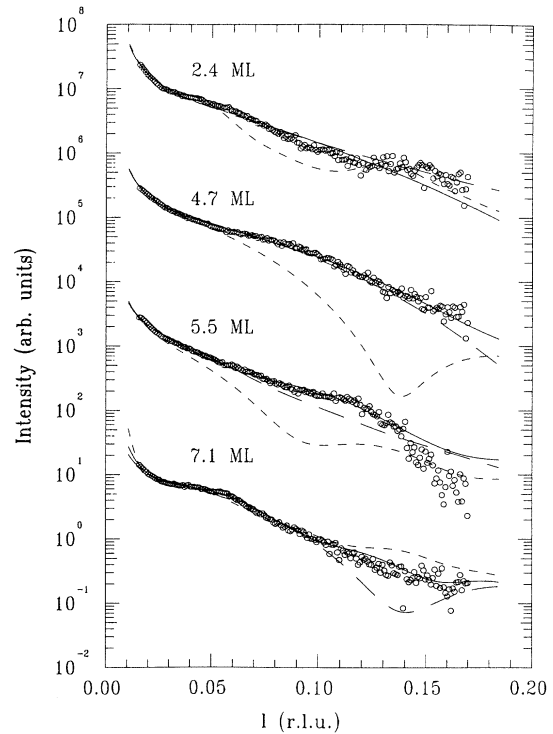


FIG. 10. Reflectivity data as a function of overlayer coverage, showing the fitted curves for the three models: Stranski-Krastanow (solid line), Volmer-Weber (small dash), and Frank-van der Merwe (large dash).

should not be given undue weight in view of the simplistic model used.

IV. CONCLUSIONS

Grazing-incidence x-ray diffraction has been employed to investigate the relaxation of strain in ultrathin films of germanium on Si(001) substrates. Radial scans in reciprocal space provide a direct measure of the strain distribution in the sample with a sensitivity unparalleled by other strain-monitoring techniques for ultrathin films. One of the important advantages of the grazing-incidence diffraction geometry is the ability to detect strain relaxation in localized regions, even when most of the overlayer is unrelaxed. By varying the grazing angle of the incident and scattered beam, the depth dependence of the strain may be probed, although the calculated penetration depths are difficult to apply if the upper surface is not flat, which occurs when islands form. X-ray reflectivity scans may also be used to monitor the morphology of the overlayer surface, thereby providing some measure of any roughness or islanding present.

The general picture that emerges from the work is that strain relaxation consistently sets in at a coverage of 3 or 4 ML, although the detailed strain distribution depends strongly on the growth conditions and thermal treatment

applied. If the amount of time the sample is exposed to high temperatures is minimized, then the extent of relaxation is slight, and the in-plane lattice parameter is close to that of the substrate. Prolonged annealing at $\approx 500^\circ\text{C}$ results in a larger change in lattice parameter, which occurs over larger regions of the layer. Increasing the growth rate from 1 ML per 18 min to 1 ML per 3 s does not suppress the onset of strain relaxation substantially under the growth conditions employed. For sample I, where the time spent at $\approx 500^\circ\text{C}$ was minimized, the amount of relaxed material increased rapidly at $\theta \approx 6$ ML. This coverage coincides with the critical coverage reported in the literature for Ge/Si(001) using ion-scattering and electron-diffraction techniques. The current data therefore indicate that these techniques detect the point at which strain relaxation propagates through large regions of the sample and that they are comparatively insensitive to limited relaxation in restricted areas. This again emphasizes the need for sensitivity in strain-relaxation measurements in order to determine the onset of relaxation.

It is now well established that growth of germanium on Si(001) proceeds in a Stranski-Krastanow mode, where islands form on the surface of the Ge at a coverage of around 3 ML, as observed by Auger spectroscopy, electron diffraction, and TEM/SEM. This coverage coincides with that at which we observe the onset of strain relaxation using grazing-incidence diffraction and of islanding from specular reflectivity measurements. This concurrence indicates strongly that strain relaxation in this system is intimately related to the islanding process, rather than to the generation of misfit dislocations. This

concurs with recent TEM observations of dislocation free islands in Ge/Si(001) for island heights of hundreds of angstrom. Recent theoretical studies of strain relaxation in Ge overlayers on Si, by energy minimization in a molecular-dynamics calculation, have also shown that it is energetically more favorable for relaxation to occur by island formation rather than the generation of misfit dislocations.³⁴ The larger islands have also been observed to grow at the expense of the smaller ones by an Ostwald ripening process as the samples were annealed. It would appear that the strain distributions observed for samples I, II, and IV reflect the distribution of strain in these islands, depending on coverage and thermal treatment. The scans at two different angles of incidence for sample I at a coverage of 11 ML therefore show that the germanium at the tops of these islands are fully relaxed, the material closer to the interface having a lattice spacing closer to that of bulk silicon.

ACKNOWLEDGMENTS

We thank J. Flapper and Th. Michielsen from the Philips Research Laboratories (Eindhoven) for providing us with accurately oriented and polished Si(001) substrates. C. Gibbings and C. Tuppen prepared the MBE grown samples (IV) and are thanked for their assistance and many discussions. Discussions with S. Jain and C. Matthai are gratefully acknowledged. This work is supported by the U.K. Science and Engineering Research Council (SERC) and the Nederlandse Organisatie voor Wetenschappelijk Onderzoek (NWO).

¹T. P. Pearsall, J. Bevk, L. C. Feldman, J. M. Bonar, J. P. Mannaerts, and A. Ourmazd, *Phys. Rev. Lett.* **58**, 729 (1987).

²G. Abstreiter, K. Eberl, E. Friess, W. Wegscheider, and R. Zachai, *J. Cryst. Growth* **95**, 431 (1989).

³J. H. van der Merwe, *J. Appl. Phys.* **34**, 123 (1962).

⁴J. W. Matthews and A. E. Blakeslee, *J. Vac. Sci. Technol.* **12**, 126 (1975).

⁵P. M. J. Marée, J. C. Barbour, J. F. van der Veen, K. L. Kavanagh, C. W. T. Bulle-Lieuwma, and M. P. A. Viegers, *J. Appl. Phys.* **62**, 4413 (1987).

⁶R. People and J. C. Bean, *Appl. Phys. Lett.* **47**, 322 (1985); **49**, 229 (1986).

⁷I. J. Fritz, *Appl. Phys. Lett.* **51**, 1080 (1987).

⁸R. H. Miles, T. C. Gill, P. P. Chow, D. C. Johnson, R. J. Hauenstein, C. W. Nieh, and M. D. Strathman, *Appl. Phys. Lett.* **52**, 916 (1988).

⁹D. C. H. Houghton, C. J. Gibbings, C. G. Tuppen, M. H. Lyons, and M. A. G. Halliwell, *Thin Solid Films* **183**, 171 (1989).

¹⁰Paul R. Berger, Kevin Chang, Pallab Bhattachaya, Jasprit Singh, and K. K. Bajaj, *Appl. Phys. Lett.* **53**, 684 (1988).

¹¹I. N. Stranski and Von. L. Krastanow, *Akad. Wiss. Lit. Mainz Math. Natur. Kl. Iib* **146**, 797 (1939).

¹²M. Volmer and A. Weber, *Z. Phys. Chem.* **119**, 277 (1926).

¹³D. J. Eaglesham and M. Cerullo, *Phys. Rev. Lett.* **64**, 1943 (1990).

¹⁴M. Zinke-Allmang, L. C. Feldman, and S. Nakahara, *Appl. Phys. Lett.* **51**, 975 (1987).

¹⁵T. Sakamoto, S. Sakamoto, K. Miki, H. Okumura, S. Yoshida, and H. Tokumoto, in *Kinetics of Ordering and Growth at Surfaces*, Vol. 239 of *NATO Advanced Study Institute, Series B: Physics*, edited by Max G. Layally (Plenum, New York, 1990).

¹⁶K. Eberl, E. Friess, W. Wegscheider, U. Menczgar, and G. Abstreiter, *Thin Solid Films* **183**, 95 (1989).

¹⁷S. A. Chambers and V. A. Loebs, *Phys. Rev. Lett.* **63**, 640 (1989).

¹⁸J. Bevk, J. P. Mannaerts, L. C. Feldman, B. A. Davidson, and A. Ourmazd, *Appl. Phys. Lett.* **49**, 286 (1986).

¹⁹S. S. Iyer, P. R. Pukite, J. C. Tsang, and M. W. Copel, *J. Cryst. Growth* **95**, 439 (1989).

²⁰A. A. Williams, J. E. Macdonald, R. G. van Silfhout, J. F. van der Veen, A. D. Johnson, and C. Norris, *J. Phys. Condensed Matter* **1**, SB273 (1989).

²¹N. Jedrecy, M. Sauvage-Simkin, R. Pinchaux, J. Massies, N. Greiser, and V. H. Etgens, *J. Cryst. Growth* **102**, 293 (1990).

²²M. Asai, H. Ueba, and C. Tatsuyama, *J. Appl. Phys.* **58**, 2577 (1985).

²³H.-J. Gossman, L. C. Feldman, and W. M. Gibson, *Surf. Sci.* **155**, 413 (1985).

²⁴M. Zinke-Allmang, L. C. Feldman, S. Nakahara, and B. A. Davidson, *Phys. Rev. B* **39**, 7848 (1989).

- ²⁵H.-J. Gossman, L. C. Feldman, and W. M. Gibson, *Phys. Rev. Lett.* **53**, 294 (1984).
- ²⁶Y.-W. Mo, D. E. Savage, B. S. Swartzentruber, and M. G. Lagally, *Phys. Rev. Lett.* **65**, 1020 (1990).
- ²⁷R. Feidenhans'l, *Surf. Sci. Rep.* **10**, 105 (1989).
- ²⁸I. K. Robinson, *Phys. Rev. B* **33**, 3830 (1986).
- ²⁹E. Vlieg, A. van't Ent, A. P. de Jong, H. Neerings, and J. F. van der Veen, *Nucl. Instrum. Methods A* **262**, 522 (1987).
- ³⁰S. S. Iyer, J. C. Tsang, M. W. Copel, P. R. Pukite, and R. M. Tromp, *Appl. Phys. Lett.* **54**, 219 (1989).
- ³¹H. Dosch, B. W. Batterman, and D. C. Wack, *Phys. Rev. Lett.* **56**, 1144 (1986).
- ³²D. A. Woolf, D. I. Westwood, and R. H. Williams, *J. Cryst. Growth* **100**, 635 (1990).
- ³³E. Vlieg, J. F. van der Veen, S. J. Gurman, C. Norris, and J. E. Macdonald, *Surf. Sci.* **210**, 301 (1989).
- ³⁴C. C. Matthai and P. Ashu, *Appl. Surf. Sci.* (to be published).